Soft Matter

Viscoplastic Fracture Transition of a Biopolymer Gel

Journal:	*Soft Matter*
Manuscript ID	SM-ART-04-2018-000722.R1
Article Type:	Paper
Date Submitted by the Author:	17-May-2018
Complete List of Authors:	Frieberg, Bradley; NIST, Materials Science and Engineering Division Garatsa, Ray-Shimry; NIST, Materials Science and Engineering Division Jones, Ronald; NIST, Materials Science and Engineering Division Bachert, John; Pfizer Consumer Healthcare, Materials and Product Chemistry Group Crawshaw, Benjamin; Pfizer Consumer Healthcare, Materials and Product Chemistry Group Liu, X.; Pfizer Consumer Healthcare, Materials and Product Chemistry Group Chan, Edwin; NIST, Materials Science and Engineering Division

Soft Matter

ARTICLE TYPE

Cite this: DOI: 10.1039/xxxxxxxxxx

Viscoplastic Fracture Transition of a Biopolymer Gel†

Bradley R. Frieberg,[a] Ray-Shimry Garatsa,[a] Ronald L. Jones,[a] John O. Bachert III,[b] Benjamin Crawshaw,[b] X. Michael Liu,[b] and Edwin P. Chan*[a]

Received Date
Accepted Date

DOI: 10.1039/xxxxxxxxxx

www.rsc.org/journalname

Physical gels are swollen polymer networks consisting of transient crosslink junctions associated with hydrogen or ionic bonds. Unlike covalently crosslinked gels, these physical crosslinks are reversible thus enabling these materials to display highly tunable and dynamic mechanical properties. In this work, we study the polymer composition effects on the fracture behavior of a gelatin gel, which is a thermoreversible biopolymer gel consisting of denatured collagen chains bridging physical network junctions formed from triple helices. Below the critical volume fraction for chain entanglement, which we confirm via neutron scattering measurements, we find that the fracture behavior is consistent with a viscoplastic type process characterized by hydrodynamic friction of individual polymer chains through the polymer mesh to show that the enhancement in fracture scales inversely with the squared of the mesh size of the gelatin gel network. Above this critical volume fraction, the fracture process can be described by the Lake-Thomas theory that considers fracture as a chain scission process due to chain entanglements.

1 Introduction

Controlling the fracture behavior of thermoreversible gels is important in a wide variety of applications such as the encapsulation and release in liquid-filled gelatin capsules, the manipulation of texture in gelled foods, as well as the stability of scaffolds in tissue engineering. Recently, it has been shown that the fracture behavior of gelatin gels is strongly deformation rate-dependent [1–3] that can be significantly enhanced by changing the viscosity of the fluid medium [3]. Unlike chemical gels that fracture via chain scission because the crosslink junctions are covalent in nature, Baumberger and coworkers suggested that the fracture process for gelatin gels can be described by a viscoplastic type process via chain disentanglement at the physical crosslinks followed by hydrodynamic frictional sliding of these disentangled chains out of "tubes" whose dimension is defined by the mesh size (ξ_M) of the gel network.

With this physical picture, a Dugdale-like cohesive zone model was derived by considering that the crack opening displacement at the fracture tip to be defined by the contour length (l) of the polymer chain when a viscoplastic stress, $\sigma(V) = \sigma_o + \sigma_{vis}(V)$, is reached. A quasi-static fracture energy term is associated with chain pull-out (σ_o), i.e. disentangled from the physical crosslinks, and a rate-dependent term that is associated with viscous drag of the disentangled polymer chains through the polymer mesh (σ_{vis}). The fracture energy ($G_c \approx \sigma(V)l$) was derived to scale as,

$$G_c \approx G_o + G_{vis} \approx \sigma_o l + \beta \eta V \left(\frac{l}{\xi_M}\right)^2 \quad (1)$$

where β is associated with the geometry of the fracture tip, η is an effective viscosity of a polymer chain in the surrounding solution and V is the fracture test velocity.

Baumberger *et al.* [3,4] demonstrated the validity of Eq. (1) for gelatin gels but focused on the effects of polymer/solvent friction on fracture for a specific gelatin composition. However, this expression suggests that the structure of the polymer chain, which defines both l and ξ_M, can also be used to control the fracture of a physical gel as it is well-established that ξ_M can be tuned simply by changing the gelatin concentration. A natural question is whether the mesh size scales with the prediction of Eq. (1). If this is indeed the case, then are there network structural length-scales that limit this viscoplastic effect? In this work, we address these questions by studying the effects of polymer network structure on the fracture behavior of gelatin gels. We show that the fracture energy of gelatin gels is strongly dependent on the volume fraction of the gelatin content. Furthermore, we demonstrate that this enhancement in the fracture energy does indeed scale with

[a] *Materials Science and Engineering Division, National Institute of Standards and Technology, Gaithersburg, MD 20899, USA. Fax: XX XXXX XXXX; Tel: XX XXXX XXXX; E-mail: edwin.chan@nist.gov*
[b] *Materials and Product Chemistry Group, Pfizer Consumer Healthcare, Richmond, VA 23220, USA.*

† Electronic Supplementary Information (ESI) available: [details of any supplementary information available should be included here]. See DOI: 10.1039/b000000x/
‡ Additional footnotes to the title and authors can be included *e.g.* 'Present address:' or 'These authors contributed equally to this work' as above using the symbols: ‡, §, and ¶. Please place the appropriate symbol next to the author's name and include a `\footnotetext` entry in the the correct place in the list.

the mesh size of the gel up to a critical gel volume fraction, beyond which the gel fractures via chain scission. We find that this critical gel volume fraction is the entanglement concentration of the gel, which is experimentally determined by studying the structure of the gelatin gels via small-angle neutron scattering.

2 Results and Discussion

For our experiments[5], gelatin gels were prepared by dissolving gelatin pellets (bovine hide, $M_n = 30.0 \pm 0.3$ kDa, $M_w = 308.7 \pm 3.2$ kDa, provided from Pfizer Consumer Healthcare) in deionized water at 70°C for several hours to form a homogeneous solution. The solution was then poured into a cylindrical mold to allow it to equilibrate and solidify overnight at room temperature. To ensure that the water content remains constant, the samples were placed inside a water vapor saturated chamber until the various measurements were conducted. Each sample was tested at room temperature ($T \approx 300$ K) in the following day to minimize the effects of aging on the mechanical property changes. We vary the gelatin/water composition in order to control the gelatin gel structure, and Table 1 summarizes the gelatin volume fractions (ϕ) investigated for this study.

Table 1 Summary of gelatin gels investigated in this study assuming density of gelatin = 1.35 g cm^{-3}.

mass % of gelatin	mass % of water	ϕ
5.0	95.0	0.038
7.5	92.5	0.057
10.0	90.0	0.076
12.5	87.5	0.096
15.0	85.0	0.116
20.0	80.0	0.156
25.0	75.0	0.198
30.0	70.0	0.241
40.0	60.0	0.330

We used contact mechanical testing (CMT) to measure the elastic modulus (E) of the gelatin gels. CMT (Fig. 1a) measures the stiffness of the gel by compressing it using a cylindrical punch, with a diameter of $2a = 3$ mm, at a fixed displacement rate ($V = d\delta/dt$). For a semi-infinitely thick gel, the stiffness is defined by the slope of the force (p) vs. displacement (δ) curve (Fig. 1a). This slope is related to the elastic modulus as $\Delta p/\Delta\delta = 2\bar{E}a$ where $\bar{E} = E/(1-\nu^2)$ is the plane-strain elastic modulus of the gel assuming a Poisson's ratio $\nu = 0.5$. The results show that E is independent of V (Fig. 1a), and we observe this rate-independence of E for all ϕ studied.

We used cavitation rheology (CR) to measure the fracture energy (G_c) of the gelatin gels. CR (Fig. 1b)[6,7] measures the critical hydrostatic pressure (P_f) imposed by a syringe needle of inner radius (r) at a constant volumetric compression rate ($\approx 0.08\,\mathrm{cm^3\,s^{-1}}$)[8] to cause the nucleation of a cavity, i.e., a reversible process or a fracture, i.e., an irreversible process, which can be discerned by the optical micrographs (Fig. 1b inset). When a reversible cavity forms, CR is quantifying the elasticity and interfacial tension (γ) of the gel, $P_f \cong \frac{5}{6}E + \frac{2\gamma}{r}$. For fracture, which occurred for all the gelatin gel formulations investigated, P_f is related to G_c and r as[9],

$$P_f \approx \left(\frac{\pi G_c E}{3}\right)^{\frac{1}{2}} \left(\frac{1}{r}\right)^{\frac{1}{2}} \quad (2)$$

We attempted to quantify the interfacial tension of low concentration gelatin solutions (≤ 2 mass %) but found that P_f is at or below the resolution of our CR instrument thus suggesting that γ is negligible for the fracture of our materials.

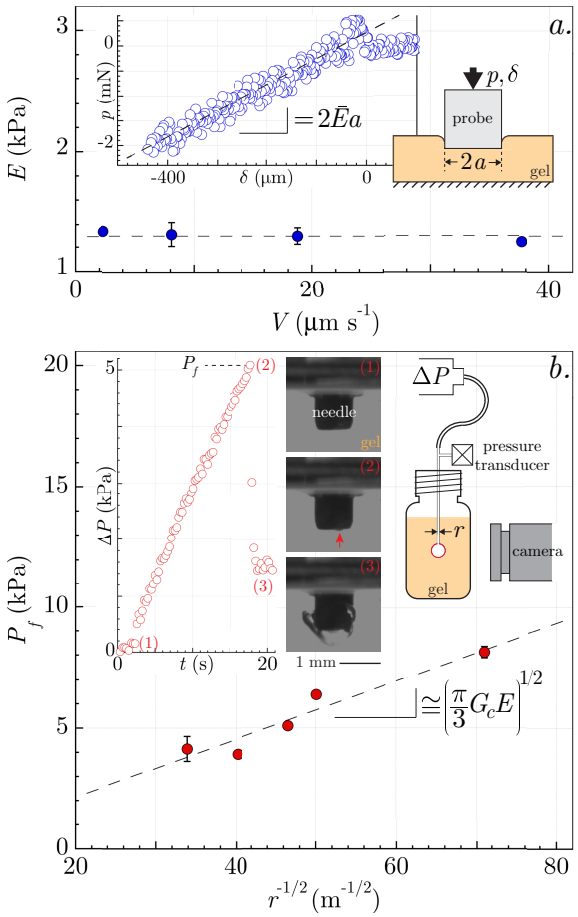

Fig. 1 Representative mechanical testing results for a gelatin gel ($\phi = 0.038$) a) The elastic modulus (E) is determined from CMT. The test involves compressing the gelatin gel with a cylindrical punch to measure the stiffness ($= \Delta p/\Delta\delta$). The results show that E is independent of the testing velocity (V). b) The fracture energy (G_c) is determined using CR, which measures the critical pressure (P_f) required to initiate fracture of the gel (inset Fig. ii). For each gel, we conduct CR at different needle diameter ($2r$) in order to determine G_c.

We do not report the CR results for $\phi = 0.33$ because P_f exceeded the pressure threshold of our CR instrument. By measuring P_f at several r (Fig. 1a), we can then use Eq. (2) to calculate G_c.

Fig. 2 summarizes the CMT and CR results as a function of ϕ. E increases with ϕ (Fig. 2a) and is consistent with the prediction for a polymer network, consisting of flexible chains, swollen in a solvent[10],

$$E \approx E_o \begin{cases} \phi^{\frac{9}{4}} & \text{for } T > \theta \\ \phi^{\frac{7}{3}} & \text{for } T = \theta \end{cases} \quad (3)$$

where $E_o \approx 1.87$ MPa is the rubbery modulus of the dry gelatin network ($\phi = 1$)[10]. The two scaling relationships describe a percolated polymer system swollen either in a good ($T > \theta$) or theta solvent ($T = \theta$). Since both scaling exponents ≈ 2.3, it is difficult to determine the solvent quality of water in gelatin simply by evaluating E vs. ϕ.

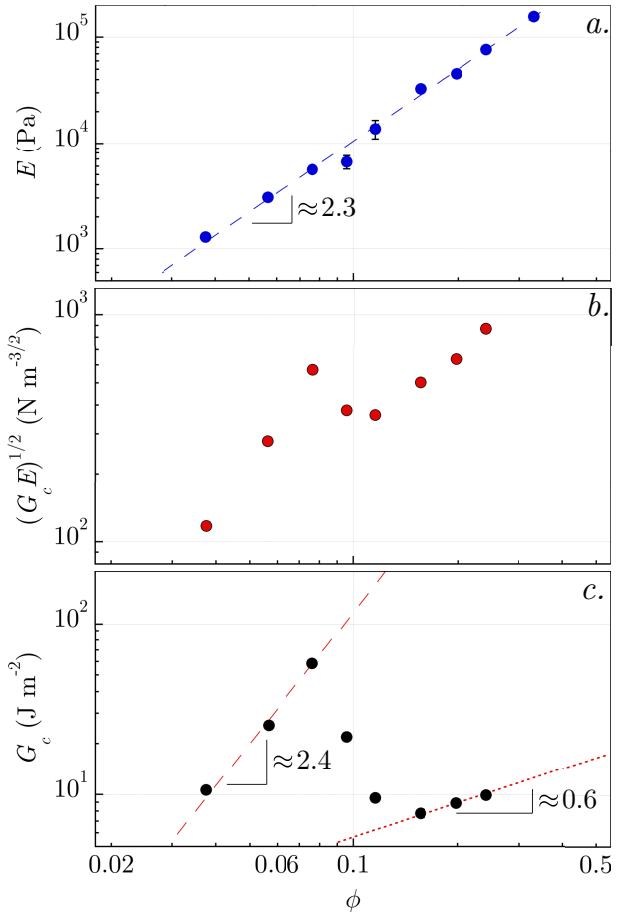

Fig. 2 Elastic modulus and fracture energy of the gelatin gels as a function of the gelatin volume fraction (ϕ). a) Elastic modulus (E) vs. ϕ as measured by CMT. b) Descriptor of fracture resistance, $(G_c E)^{\frac{1}{2}}$, as a function of ϕ as measured by CR. c) G_c vs. ϕ.

The parameter $(G_c E)^{\frac{1}{2}}$ obtained from CR serves as a descriptor of the critical pressure for fracture that is normalized by the initial cavity or flaw size as defined by r. In general, it shows an increase with increasing ϕ (Fig. 2b). We convert this parameter to G_c using the E values to find that G_c is not a constant value for all ϕ nor does it increase in a monotonic fashion similar to E (Fig. 2c). Instead, we can be separate the scaling between G_c and ϕ into 2 distinct regions. For $\phi \lesssim 0.08$, we find that $G_c \approx \phi^{2.4}$ and reaches a maximum value of ≈ 60 J m^{-2} at $\phi = 0.076$. We note that this power-law scaling for G_c, with a similar power-law exponent, has been observed previously for different gelatin gels using other fracture testing approaches[11,12]. For $\phi \geq 0.156$, $G_c \approx \phi^{0.6}$, but the values are significantly lower than that of the first region.

To understand the fracture behavior of these two regions, we use small-angle neutron scattering (SANS) to characterize the structure of the D_2O swollen gelatin gels as a function of ϕ. The scattering intensity ($I(Q)$) vs. Q results (Fig. 3a) are fitted using the correlation length scattering model, $I(Q) = A/Q^m + C/(1+(Q\xi)^n) + B$[13]. The first term of this expression is the Porod function describing the clustering of the gel structure at large length-scales with the Porod exponent m characterizing the fractal nature of the gel and B is the incoherent background. The second term is the Lorentzian function that characterizes the thermodynamics of the gelatin/water system. Specifically, the Lorentzian exponent (n) is the inverse of the Flory exponent ($\nu_F = 1/n$)[13] and ξ is the correlation length of the polymer chains. Table 2 summarizes the fitting parameters for the SANS results using this scattering model.

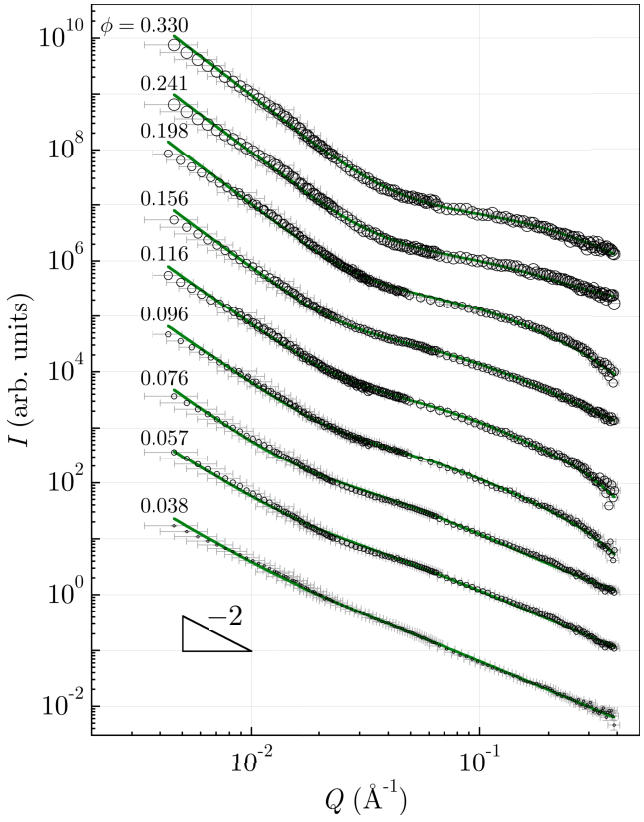

Fig. 3 SANS results of the gelatin gels. Scattering intensity (I) vs. scattering vector (Q) of the gelatin gels dissolved in D_2O. The circles are the experimental results and the curves are the fits to the data using the correlation length scattering model, $I(Q) = A/Q^m + C/(1+(Q\xi)^n) + B$.

Table 2 Fitting parameters (m, n, ξ), with fitting uncertainties, and calculated ν_F values obtained from the SANS results using the correlation length scattering model, $I(Q) = A/Q^m + C/(1+(Q\xi)^n) + B$.

ϕ	m	n	ξ (Å)	$\nu_F = 1/n$
0.038	2.47 ± 0.18	1.66 ± 0.02	47.9 ± 8.7	0.60
0.057	2.64 ± 0.08	1.72 ± 0.03	38.6 ± 2.5	0.58
0.076	2.95 ± 0.04	1.91 ± 0.03	31.0 ± 0.9	0.52
0.096	2.88 ± 0.04	1.85 ± 0.04	20.9 ± 1.1	0.54
0.116	2.93 ± 0.03	1.94 ± 0.04	15.6 ± 0.6	0.52
0.156	3.07 ± 0.03	1.97 ± 0.04	14.3 ± 0.5	0.51
0.198	3.15 ± 0.01	2.00 ± 0.02	10.8 ± 0.1	0.50
0.241	3.10 ± 0.02	2.00 ± 0.03	8.1 ± 0.2	0.50
0.330	3.16 ± 0.02	1.87 ± 0.05	5.6 ± 0.2	0.53

The correlation lengths presented in Table 2 quantify the mesh size (ξ_M) of the gelatin gels, and show a decrease in ξ_M with increasing ϕ (Fig. 3a). Additionally, Table 2 indicates that ν_F, which is a measure of the solvent quality, changes with ϕ. For $\nu_F > 0.5$, water is a good solvent for gelatin for $\phi \leq 0.08$ whereas for $\phi > 0.08$, $\nu_F \approx 0.5$ and this is consistent with that of a θ-solvent. According to scaling relationships for flexible polymers in solution[10,14], the chain dimensions should scale with ϕ and ν_F as,

$$\xi \approx \begin{cases} R_F\left(\frac{\phi^*}{\phi}\right)^{\frac{3}{4}} = b\left(\frac{\mathrm{v}}{b^3}\right)^{-\frac{1}{4}}\phi^{-\frac{3}{4}} & \text{for } T > \theta \\ b\phi^{-1} & \text{for } T = \theta \end{cases} \quad (4)$$

where R_F is the size of the gelatin chain in a good solvent, b is the Kuhn length of the gelatin chain and $\mathrm{v} = (1-2\chi)b^3$ is the excluded volume parameter.

We use Eq. (4) to fit the results of Fig. 4a by considering that the critical volume fraction (≈ 0.08) is the critical volume fraction (ϕ_e) that delineates a semi-dilute unentangled polymer solution versus an entangled polymer solution. Intrinsic viscosity measurements of gelatin solution show that $[\eta] = 0.45$ dL g^{-1} thus implying that all of the gelatin gels studied are above the overlap concentration since $c^* \cong \frac{\nu}{\alpha^3 N^{\frac{1}{2}} b^3} = \frac{1.5}{[\eta]} = 0.033$. This implies that the overlap volume fraction, $\phi^* \cong 0.024$, which is the critical volume fraction that defines the crossover between dilute and semi-dilute polymer solution regimes[15]. The gelatin gel is considered an entangled polymer for $\phi > \phi_e$, whereas it is considered to be an unentangled gel for $\phi \leq \phi_e$.

The change in ξ vs. ϕ as measured by SANS is schematically represented in Fig. 4b and Fig. 4c. Experimentally, we find that gels are formed across the entire range of ϕ investigated. For $\phi \leq \phi_e$, $\xi \approx \xi_M$ since the SANS results show that $\nu > 0.5$ thus excluding volume interactions are not screened. For $\phi > \phi_e$, $\nu \approx 0.5$, which means that the chains are overlapped with neighboring chains and ξ is no longer measuring the distance between crosslinked junctions but rather portions of the chain between entanglement points. We use the $\phi > \phi_e$ region to find that $b \approx \xi\phi = 2.2$ Å. To determine the Flory interaction parameter (χ), we use the $\phi \leq \phi_e$ region to find that $\chi \approx \frac{(1-(b/\xi)^4)}{2} = \frac{(1-(2.2\,\text{Å}/4.3\,\text{Å})^4)}{2} = 0.466$ thus confirming that water is a good solvent for gelatin when $\phi \leq \phi_e$.

Our proposed structural model is different from the previously proposed structural model for gelatin gels. Based on rheological measurements, Joly-Duhamel and coworkers suggested that the structure of gelatin gel is analogous to actin gels, and consists of an entangled network of rigid rods that are deformable at the flexible network junctions[16]. If this was indeed the case for our materials, the SANS results will show $I(Q) \sim Q^{-1}$ scaling yet Fig. 3a does not display such scaling. Furthermore, Kratky analysis of the SANS results show that the structure of our gelatin gels is not consistent with this rod-like model (Supplemental info, Fig. S1). This is also supported by the CMT results. For a polymer network with semi-flexible rods, $E \sim \phi^{\frac{7}{5}}$ since the elasticity is now related to the bending energy of the rod[17]. However, we find that E for our materials (Fig. 2) has a significantly stronger ϕ dependence for all gelatin gels investigated. All of these results

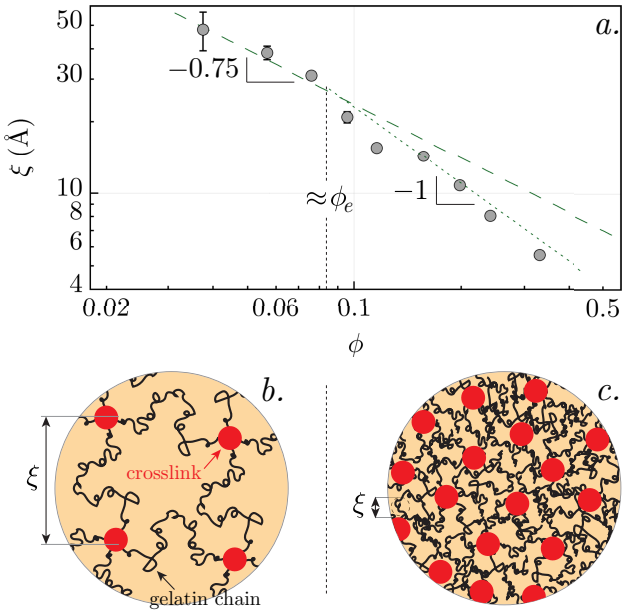

Fig. 4 a) Correlation length (ξ) vs. ϕ of the gelatin gels. The curves are fitted using the two scaling relationship as defined by Eq. (4), which depends on the solvent quality. Schematic representation of the gelatin gel structure for b) $\phi \leq \phi_e$, and c) $\phi > \phi_e$.

confirm that the structure of our gelatin gels is consistent with a polymer network consisting of flexible chains between crosslink junctions.

Now that we have established the scaling relationships of the gelatin chains as a function of ϕ, we now revisit the G_c vs. ϕ results (Fig. 2c). The Lake-Thomas theory[18] is the classic model used to describe the fracture energy of polymer gels, $G_c \approx \Gamma N U$, where Γ is the areal density per unit area of the polymer chains that crosses the fracture plane, $\Gamma \approx \xi^{-2}$. N is the number of monomers that are involved in the fracture process when a covalent bond breaks as quantified by the bond dissociation energy, U. In addition to solvent quality, the presence of chain entanglements, defined as N_e, will affect the scaling for N,

$$N \approx \begin{cases} \phi^{-\frac{5}{4}} & \text{for } T > \theta, N < N_e \\ \phi^{-\frac{4}{3}} & \text{for } T = \theta, N > N_e \end{cases} \quad (5)$$

Substituting Eq. (4) and Eq. (5) into the Lake-Thomas fracture energy expression, we obtain the following based on schematic of the gelatin structure presented in Fig. 4b and Fig. 4c,

$$G_c \approx \Gamma N U \approx \frac{U}{b^2}\begin{cases} (1-2\chi)^{\frac{1}{2}}\phi^{\frac{1}{4}} & \text{for } \phi \leq \phi_e \\ \phi^{\frac{2}{3}} & \text{for } \phi > \phi_e \end{cases} \quad (6)$$

We see that Eq. (6) agrees well with the results of Fig. 2c for $\phi > \phi_e$. Using the quantitative fracture energy expression of the Lake-Thomas theory[19], we predict $G_c = (27/8)^{\frac{1}{2}} U b^{-2} \approx 22$ J m^{-2} assuming the bond dissociation energy of a carbon-carbon bond ($U = 350$ KJ mol^{-1}) with $b = 2.2$ Å. This value is in excellent agreement with the extrapolated value of $G_c \approx 26$ J m^{-2} at $\phi = 1$.

However, Eq. (6) does not agree at all with the results of Fig. 2c for $\phi \leq \phi_e$ both in terms of the absolute magnitude of G_c as well as the scaling with ϕ. This suggests that the Lake-Thomas theory

does not properly capture the mechanism of fracture for these materials at low gelation concentration.

Recent works by Baumberger and coworkers[3,4] demonstrated the applicability of Eq. (1) for describing the fracture behavior of gelatin gels. Following chain pullout of the crosslink junctions as described by G_o, these disentangled chains then move through the polymer mesh that can be effectively treated as tubes with diameter ξ_M. This can be viewed as a poroelastic process, where $\xi_M \cong (D_c\eta/E)^{\frac{1}{2}}$ [20,21]. D_c is the cooperative diffusion coefficient of the polymer chain in solution and η is the solvent viscosity[22]. Substituting this relationship and Eq. (3) into Eq. (1), the fracture energy associated with this process is,

$$G_{vis}(V) \approx \frac{\beta V l^2 E}{D_c} \approx \frac{4\beta V l^2 k_B T}{D_c b^3}\phi^{\frac{9}{4}} \tag{7}$$

The scaling prediction of $G_{vis} \sim E$ from Eq. (6) is consistent with our results in Fig. 5 when $\phi \leq \phi_e$, whereas there is no correlation between G_c and E when $\phi > \phi_e$. Since we are studying the fracture behavior of one type of gelatin material at a fixed deformation rate, l and E_o are fixed by the molecular structure of the specific gelatin, while β and V can be treated as constants defined by the CR testing conditions. D_c is the remaining parameter this is concentration dependent. Depending on whether a polymer solution is dilute or semi-dilute, D_c can be independent of the polymer concentration ($D_c \sim \phi^0$) or concentration-dependent ($D_c \sim \phi^{-\frac{3}{4}}$ to $\sim \phi^{-1}$)[22,23]. Diffusion measurements on gelatin solutions have demonstrated that D_c can range from being concentration independent ($D_c \sim \phi^0$)[2] to weakly concentration dependent ($D_c \sim \phi^{\frac{3}{10}}$)[24], thus G_{vis} can scale from $\sim \phi^{\frac{9}{4}}$ to $\sim \phi^{\frac{51}{20}}$. The fact that $G_c \sim \phi^{2.4}$ (Fig. 2c) suggests that $D_c \sim \phi^{\frac{1}{10}}$ for our gelatin gels. A possible explanation for this weak concentration dependence, given that $\phi > \phi^*$, is the significant polydispersity (PDI ≈ 10) of the gelatin polymer. This polydispersity effect may also explain the broadness in the transition of the fracture mechanisms for $\phi_e < \phi < 0.156$ (Fig. 2c) in defining the specific value of ϕ_e. However, this question is beyond the scope of the current study as understanding this broadness requires reducing the polydispersity via fractionation of the polymer.

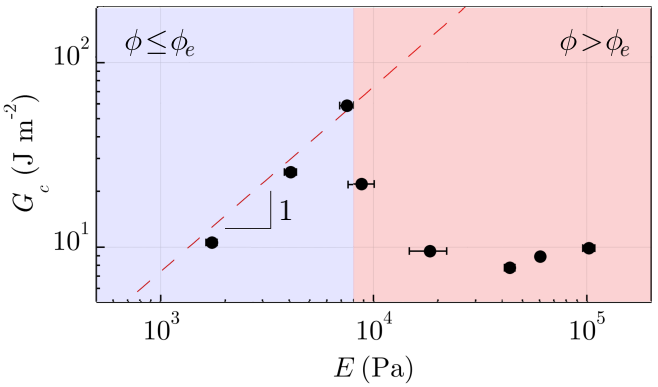

Fig. 5 Comparison of fracture energy (G_c) and elastic modulus (E) of the gelatin gels.

3 Conclusions

In conclusion, we have demonstrate that the fracture energy of gelatin gels can be significantly enhanced by leveraging this viscoplastic process. The entanglement concentration defines the transition between this viscoplastic fracture mechanism versus the chain scission mechanism of fracture as captured by the Lake-Thomas theory. For $\phi \leq \phi_e$, the gelatin gel is considered to be below the chain entanglement solution concentration and viscoplastic mechanism of fracture appears to be the primary mechanism of fracture. For $\phi > \phi_e$, the gel is sufficiently concentrated such that the chains are entangled with each other and the primary mechanism of fracture is chain scission since these topological constraints prevent the viscoplastic process.

There are several questions we will address in the future in regards to gaining a better understanding of the viscoplastic fracture model. The first is whether chain pullout of the crosslink junctions occurs prior to the viscoplastic process since there is likely a fraction of "free" chains that are not part of the network that can already participate in this viscoplastic process without having chain pullout to occur. The second is the velocity dependence for Eq. (7). Given that it is difficult to vary V significantly using CR, we are developing other fracture tests to investigate this velocity dependence for gelatin gels. The third question is the application of this viscoplastic mechanism of fracture to control the properties of gelatin gels and other physical gels. Eq. (1) suggests that there are several materials strategies to maximize this viscoplastic effect. One mechanism is by adjusting η. As demonstrated by Baumberger *et al.*[3], an increase in solvent viscosity leads to a proportional enhancement in G_c as it increases the hydrodynamic friction between the polymer chain and the surrounding solvent. Thus future fracture studies will be focused on studying the effects of incorporating viscous fluids to these gels. Another approach of enhancement is to increase ϕ_e in order to extend the phase space where viscoplasticity is dominant. This strategy is less straightforward compared to the first one as this most likely requires designing new polymer network architectures that can reduce chain entanglements although new polymer architectures such as bottlebrush networks[25] can be potentially interesting.

Pertaining to gelatin gels used as liquid-filled capsules, the release of the drug occurs when the gel ruptures due to an internal pressure buildup. Thus $(G_cE)^{\frac{1}{2}}$, which is effectively the stress intensity factor, can be used as a descriptor of the rupture resistance due to this applied pressure. The results in Fig. 2b show that the contributions from elasticity vs. viscoplasticity on the rupture resistance of a capsule will vary depending on the specific gelatin concentration. Although the highest gelatin content resulted in the highest measured value for the rupture resistance and would suggest that one should focus on increasing the elasticity of the gelatin to improve rupture resistance, our results indicate that viscoplasticity can play a very significant role in the rupture resistance of a physical gel especially when $\phi \approx \phi_e$ or by modifying the elastic and fracture properties of the gel via addition of viscous fluids.

Acknowledgements

R.S.G. acknowledges the NIST Summer Undergraduate Research Fellowship (SURF) for financial support. The authors thank the NIST Center for Neutron Research for access to neutron scattering facilities. E.P.C. thank Prof. Emanuela Del Gado of Georgetown and Dr. Edmund "Pete" Maziarz of Pfizer for insightful discussions, as well as Dr. Christopher L. Soles for critical reading of the manuscript. This work is a contribution of NIST, an agency of the U.S. Government, and not subject to U.S. copyright.

References

1 A. Takada, *J. Geophys. Res.*, 1990, **95**, 8471–8481.

2 T. Baumberger, C. Caroli and O. Ronsin, *Eur. Phys. J. E.*, 2003, **11**, 85–93.

3 T. Baumberger, C. Caroli and D. Martina, *Nat. Mater.*, 2006, **5**, 552–555.

4 T. Baumberger, C. Caroli and D. Martina, *Eur. Phys. J. E.*, 2006, **21**, 81–89.

5 *Certain instruments and materials are identified in this paper to adequately specify the experimental details. Such iden- tification does not imply recommendation by the National Institute of Standards and Technology; nor does it imply that the materials are necessarily the best available for the purpose.*

6 J. A. Zimberlin, N. Sanabria-DeLong, G. N. Tew and A. J. Crosby, *Soft Matter*, 2007, **3**, 763–767.

7 S. Kundu and A. J. Crosby, *Soft Matter*, 2009, **5**, 3963.

8 S. M. Hashemnejad and S. Kundu, *Soft Matter*, 2015, **11**, 4315–4325.

9 Y. Y. Lin and C. Y. Hui, *Int. J. Fract.*, 2004, **126**, 205–221.

10 M. Rubinstein and R. H. Colby, *Polymer Physics*, Oxford University Press, USA, 1st edn, 2003.

11 A. E. Forte, F. D'Amico, M. N. Charalambides, D. Dini and J. G. Williams, *Food Hydrocoll.*, 2015, **46**, 180–190.

12 M. Czerner, L. A. Fasce, J. F. Martucci, R. Ruseckaite and P. M. Frontini, *Food Hydrocoll.*, 2016, **60**, 299–307.

13 B. Hammouda, D. L. Ho and S. Kline, *Macromolecules*, 2004, **37**, 6932–6937.

14 S. T. Milner, *Macromolecules*, 2005, **38**, 4929–4939.

15 I. Teraoka, *Polymer Solutions: An Introduction to Physical Properties*, 2002.

16 C. Joly-Duhamel, D. Hellio, A. Ajdari and M. Djabourov, *Langmuir*, 2002, **18**, 7158–7166.

17 C. Broedersz and F. MacKintosh, *Rev. Mod. Phys.*, 2014, **86**, 995–1036.

18 G. J. Lake and A. G. Thomas, *Proc. R. Soc. Lond. A*, 1967, **300**, 108–119.

19 Y. Akagi, H. Sakurai, J. P. Gong, U.-i. Chung and T. Sakai, *J. Chem. Phys.*, 2013, **139**, 144905.

20 E. P. Chan, Y. Hu, P. M. Johnson, Z. Suo and C. M. Stafford, *Soft Matter*, 2012, **8**, 1492–1498.

21 E. P. Chan, B. Deeyaa, P. M. Johnson and C. M. Stafford, *Soft Matter*, 2012, **8**, 8234–8240.

22 P. G. De Gennes, *Macromolecules*, 1976, **9**, 587–593.

23 U. Zettl, M. Ballauff and L. Harnau, *J. Phys.: Condens. Matter*, 2010, **22**, 494111.

24 E. J. Amis, P. A. Janmey, J. D. Ferry and H. Yu, *Macromolecules*, 1983, **16**, 441–446.

25 J. M. Sarapas, E. P. Chan, E. M. Rettner and K. L. Beers, *Macromolecules*, 2018, **51**, 2359–2366.